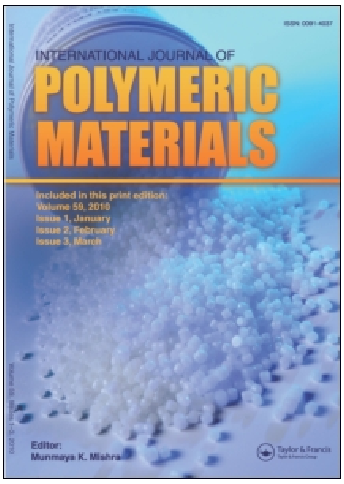

International Journal of Polymeric Materials
Publication details, including instructions for authors and subscription information:
http://www.informaworld.com/smpp/title~content=t713647664

Redox-Initiated Bulk Polymerization of Methyl Methacrylate Using a CuO/TiO_2 Catalyst System

Sanaa M. Solyman[a]; Salah A. Hassan[b]; Salwa A. Sadek[b]; Hesham S. Abdel-Samad[b]
[a] Department of Petrochemical Technology, Egyptian Petroleum Research Institute, Nasr City, Cairo, Egypt [b] Department of Chemistry, Faculty of Science, Ain Shams University, Abbassia, Cairo, Egypt

To cite this Article Solyman, Sanaa M. , Hassan, Salah A. , Sadek, Salwa A. and Abdel-Samad, Hesham S.(2010) 'Redox-Initiated Bulk Polymerization of Methyl Methacrylate Using a CuO/TiO_2 Catalyst System', International Journal of Polymeric Materials, 59: 7, 475 — 487

To link to this Article: DOI: 10.1080/00914031003627072

URL: http://dx.doi.org/10.1080/00914031003627072

International Journal of Polymeric Materials, 59:475–487, 2010
Copyright © Taylor & Francis Group, LLC
ISSN: 0091-4037 print/1563-535X online
DOI: 10.1080/00914031003627072

Redox-Initiated Bulk Polymerization of Methyl Methacrylate Using a CuO/TiO_2 Catalyst System

Sanaa M. Solyman,[1] Salah A. Hassan,[2] Salwa A. Sadek,[2] and Hesham S. Abdel-Samad[2]

[1]Department of Petrochemical Technology, Egyptian Petroleum Research Institute, Nasr City, Cairo, Egypt
[2]Department of Chemistry, Faculty of Science, Ain Shams University, Abbassia, Cairo, Egypt

Catalytic bulk polymerization of methyl methacrylate (MMA) has been carried out at 80°C over pure titania (anatase), and supported CuO/TiO_2 catalyst system of different CuO % loadings (ranged between 0.5–20 wt%), without using an initiator or cocatalyst. The produced polymers were characterized via hydrogen nuclear magnetic resonance (^{1}HNMR) and gel permeation chromatography (GPC). The prepared catalyst samples were characterized by thermogravimetric analysis (TGA), X-ray diffraction (XRD), Fourier transform infrared (FTIR), scanning electron microscopy (SEM), transmission electron microscopy (TEM) and N_2-adsorption-desorption. The polymer yield (%) was shown to increase by increasing the CuO content up to 8.0 wt%, and then decreased. All polymers were of high molecular weights with low % of pentads. They were almost of syndiotactic-rich structure, produced mainly through a chain-end control mechanism. The polymerization process was suggested to be catalyst-dependent, redox-initiated and following a free radical mechanism. The sample of 8.0% CuO loading (above the monolayer coverage) was the most active; a fraction of loaded CuO existed on the titania external surface, while a larger fraction seemed to be inserted into the support pore system.

Keywords bulk polymerization, CuO/TiO_2 catalyst system, MMA, redox-initiated

---

Received 14 December 2009; in final form 21 December 2009.

Address correspondence to Sanaa M. Solyman, Department of Petrochemical Technology, Egyptian Petroleum Research Institute, Nasr City, Cairo, Egypt. E-mail: sanaa8763@hotmail.com

INTRODUCTION

Titanium dioxide has attracted a considerable interest for its applications in photocatalysis [1,2], solar energy cells, ductile ceramics, the pigment industry, optical and optoelectronic devices [3]. Titania exists in three types of crystalline forms, namely rutile, anatase and brookite, among which anatase is specically recognized in several catalytic applications [4–6]. Several catalyst systems in use involve metals and metal oxides supported on high-surface-area anatase. The role of titania was considered rather more complex than expected to increase the catalyst surface area and the active phase-TiO_2 interactions, affecting the reactivity and selectivity [7]. Although TiO_2 was not much suitable as a structural support material for metals compared with Al_2O_3 and SiO_2, small additions of TiO_2 were found to modify metal-based catalysts to a significant extent. Moreover, the OH groups on the titania surface could be used as anchoring sites for the attachment of many covalently bound surface modifiers, or coupling agents such as organosilanes, metal alkoxides, epoxides, and isocyanates [8–10]. On the other hand, although pure copper metal, copper oxide and copper salts have been tested in the polymerization of MMA in different media [11], the performance of supported CuO on titania in the polymerization process, particularly in controlling behavior through the enchainment, seems obviously lacking in the literature. The present study was thus undertaken to follow up the bulk polymerization of MMA at 80°C in the presence of CuO/TiO_2 system, of different CuO loadings, without using an activator or cocatalyst. The produced polymers were characterized through GPC and ^{1}HNMR investigation. Full characterization of the solid catalyst samples was carried out through XRD, FTIR, TGA, SEM, TEM and N_2 adsorption techniques. The enchainment and the stereoregularity of the produced polymers were investigated and are discussed at the studied conditions.

EXPERIMENTAL

Catalyst

The different samples of supported copper oxide on TiO_2 (anatase) were prepared by impregnation of the preweighed amount of TiO_2 with a basic copper carbonate ($CuCO_3$ Cu $(OH)_2 \cdot H_2O$, BDH grade) solution of an appropriate concentration. The mixture was stirred for 3 h thoroughly to homogeneity and gradually dried at 110°C for 4 days. The dried product was then subjected to calcination at 360°C for 4 h in air. This temperature was chosen on the basis of data obtained by TGA analysis of pure basic copper carbonate and a precalcinated sample of basic copper carbonate-supported TiO_2 (15CuT), showing considerable thermal stabilities at $t > 320°C$ (Figure 1) [1]. The prepared

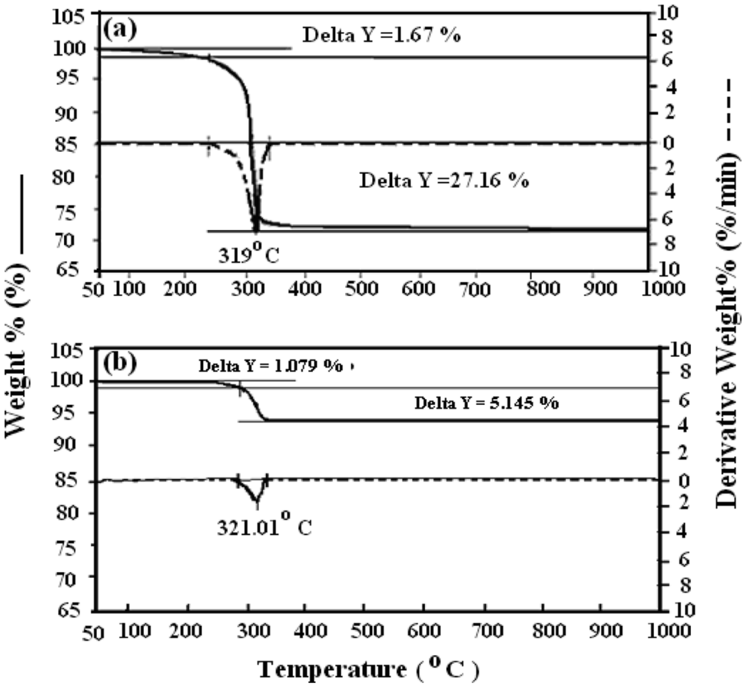

Figure 1: TGA of basic copper carbonate (a) and a precalciened catalyst sample of 15CuT (b).

catalyst samples were designated as xCuT, where x corresponds to CuO loadings of 0.5, 2.0, 8.0, 15 and 20 wt% on titania surface.

Catalyst Characterization

XRD patterns for various samples under study were recorded by the aid of a Philips X' Pert MPP diffractometer with a geniometer of type PW 3050/10 using nickel-filtered CuKα radiation ($\lambda = 1.5406$). FTIR measurements were performed by using Thermo Scientific, Nicolet 6700 spectrophotometer at a resolution 5.3 cm^{-1} over the wave numbers 4000–450 cm^{-1}. Thermogravimetric analysis (TGA) of original $CuCO_3 \cdot Cu(OH)_2 \cdot H_2O$ precursor and a precalcined catalyst sample of 15CuT was carried out in the presence of static air at a heating rate of 10°C min^{-1} using a Perkin Elmer Thermal Analyzer. Morphology of different samples was studied by means of TEM, Jeol 1200 EXII, resolution 0.2 nm, 120 KV) as well as by SEM on a JEOL JSM-5300 instrument working at 30 KV. The texture of the samples was investigated by measuring the specific surface area (S$_{BET}$) followed by pore size analysis, based on adsorption – desorption isotherms of N_2 at −196°C [12].

Bulk Polymerization of Methyl Methacrylate (MMA)

Stabilized MMA was purified by shaking with 20% NaOH solution to remove the quinine inhibitor, followed by washing several times with bidistilled water and then with ammonium acetate for neutrality. The product was dried over $CaCl_2$, vacuum distilled, and stored at about 6°C over anhydrous sodium sulphate [13,14].

The catalytic activity of various samples was measured in the bulk polymerization of MMA as follows: The freshly distilled stabilizer-free monomer (2.8 g) [13,14] was introduced into the polymerization tube (20 ml capacity) together with a weighed sample of the catalyst (0.06 g), of different CuO loadings. The reaction mixture was deaerated by passing pure dry nitrogen, and then the reaction tube was sealed and placed in a thermostated water bath adjusted at 80°C for 5 h. After cooling to room temperature, the tube was carefully opened and the content was dissolved in acetone with occasional shaking. The solution was filtered to separate the catalyst and the filtrate was run in methanol to precipitate the polymer (10 ml of alcohol for each 1 ml of the reaction mixture). The produced polymer was filtered and dried under vacuum at 40°C till constant weight. The polymer yield (or % conversion) was then calculated as follows:

$$\text{Polymer yield (Y\%)} = (\text{weight of the produced polymer/weight of monomer}) \times 100.$$

Characterization of Poly Methylmethacrylate (PMMA)

Molecular weight distribution analysis of the produced polymer was carried out through GPC analysis. The measurements were performed in toluene of HPLC grade as the mobile phase with a rate of elution, 0.7 ml min^{-1} at 40°C. Molecular weights were determined relative to monodisperse polystyrene standards. Calculations were performed using the Millennium 32 Chromatography Manager with gel-permeation application software. ^{1}HNMR spectra of the products were obtained on a Bruker-300 MHz spectrometer with a superconducting magnet and 5 mm dual-probe head. Duterated chloroform ($CDCl_3$) was used as the solvent and tetramethylsilane as an internal reference.

RESULTS AND DISCUSSION

X-Ray Diffraction Analysis (XRD)

Figure 2 shows XRD patterns of pure TiO_2 anatase (a), CuO (b) and supported samples xCuT with loadings ranged between 0.5 and 20.0 wt% (c, d, e, f and g, respectively). For pure TiO_2 support, the obtained pattern shows

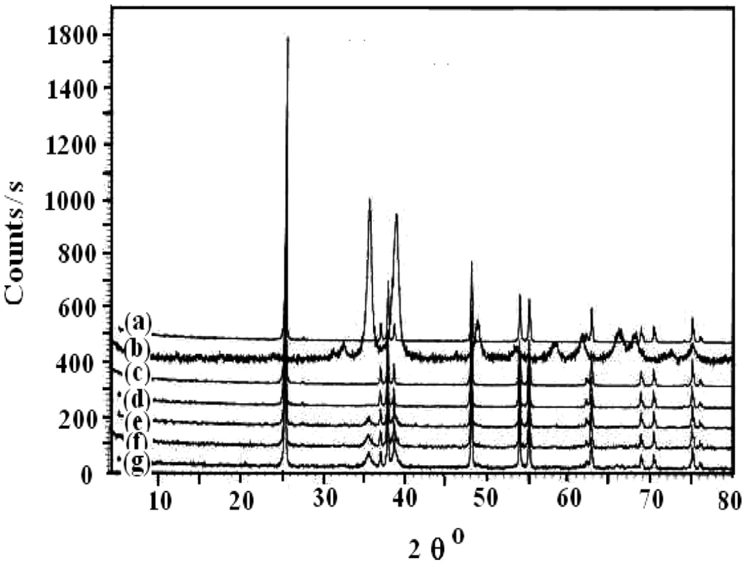

Figure 2: XRD patterns of parent TiO_2 (a), CuO (b), and different supported samples of CuO/TiO_2: 0.5CuT (c), 2CuT (d), 8CuT (e), 15CuT (f), and 20CuT (g).

the main peaks at 2θ (and d-spacing) as follows: 25.32° (3.5Å), 36.96° (2.43 Å), 37.78° (2.37 Å) 38.58° (2.33 Å) 48.03° (1.89 Å), 53.88° (1.69 Å) and 55.06° (1.66 Å) [1,2,15]. For pure CuO, the obtained pattern shows the main characteristic peaks of pure CuO at 2θ (and d-spacing) as follows: 35.5° (2.53 Å), 38.7° (2.31 Å) and 48.7° (1.86 Å) corresponding to ($^{-}111$), (111) and ($^{-}202$) reflections, respectively *(JCPDS File No. 05-0661)* [1,2,16]. From the XRD patterns of the diluted samples (0.5CuT and 2CuT), no characteristic peaks of CuO could be detected, which might be due to the small-sized particles of CuO that exist in high dispersion on the titania surface. For the more concentrated samples (8CuT–20CuT), the characteristic peaks of CuO crystallites could be observed, intensities of which were enhanced by increasing the % loading [1]. These results coincided with previous observations [17] that CuO can be highly dispersed as a monolayer on TiO_2 anatase, where the monolayer dispersion threshold of CuO on TiO_2 was 5.1 mg CuO/1 g TiO_2 (i.e., 5.1 wt%). By analysis of our obtained XRD data, the average crystallite sizes of the CuO in supported samples ($D_{av.}$) were estimated through the Scherrer's equation, $D_{av.} = K\lambda/\beta \cos\theta$, where λ is the X-ray wavelength, β the breadth of diffraction rays due to the crystallite size, θ the Bragg's angle of diffraction and K is a constant [18]. The calculated D_{av} values in Table 1 show a maximum increase in the crystallite size for the sample of 8CuT (viz., 63.5 nm). With a further increase of the CuO content, the gradual decrease in $D_{av.}$ may be referred to increased surface migration of some copper oxide species [19].

Table 1: The average crystallite size ($D_{av.}$ nm) for pure CuO and CuO supported on TiO_2 in different loadings calculated from XRD analysis and various surface parameters of pure TiO_2 and various catalyst samples of different CuO loadings.

Sample	$D_{av.}$ (nm) from XRD	C_{BET}	S_{BET} (m^2/g)	S_t (m^2/g)	V_p (ml/g)	r^{-cp} (nm)
Pure CuO	30.08	–	–	–	–	–
Pure Titania(T)	–	75	27.7	28	0.4073	14.7
0.5CuT	–	251	34.5	40	0.3521	10.2
2CuT	–	211	41.0	46	0.3210	7.8
8CuT	63.47	93	66.4	67	0.3106	4.7
15CuT	43.30	31	92.5	97	0.2968	3.2
20CuT	35.40	142	61.1	64	0.2658	4.4

FTIR Spectroscopic Analysis

The FTIR spectra of various supported samples (xCuT) are shown in Figure 3. For comparative study, analysis will be focused on the main characteristic peaks of TiO_2 (508 and 670 cm^{-1} [15]) and that of CuO [16] (503 and 521 cm^{-1}). Upon supporting CuO on TiO_2, in the dilute samples (0.5CuT and 2CuT), the main characteristic peaks of TiO_2 are observed with little shift (spectra a, b). For the other catalyst samples of loadings ≥8 wt% CuO, the characteristic peak of CuO at 503 cm^{-1}, overlapped with that of TiO_2 at 508 cm^{-1}, becomes much more pronounced with the increase in CuO loading. Moreover, the characteristic peak of CuO at 521 cm^{-1} seems to suffer some shift, from 521 cm^{-1} to 544 cm^{-1}, pointing to the interaction and/or clustering of the CuO phase on the TiO_2 surface. The interaction may be confirmed by the appearance of a new weak peak at 892.5 cm^{-1}, not common for CuO or TiO_2. Observed splitting in this band may be linked with the change in the modes of interaction.

Scanning Electron Microscope (SEM) and Transition Electron Microscope (TEM)

The SEM images of pure TiO_2 and various xCuT samples with different loadings are shown in Figure 4. The images indicate that the addition of CuO on a TiO_2 surface could affect the catalyst surface morphology. It can be evident that CuO/TiO_2 systems under study constituted aggregated particles with relatively uniform sizes [1,2]. For 8CuT and 15CuT samples (Figure 4(d) and (e)), surface decoration is evidenced, as a result of surface migration of CuO species and possible favored interaction mode between CuO and titania phases. An image was taken for 8CuT by TEM (Figure 4(f)). This image indicates the presence of the majority of CuO crystallites as dark specks on TiO_2 particles. For more clearance, another image with a higher magnification factor was taken (the inset image in Figure 4(f)) which confirms the decoration

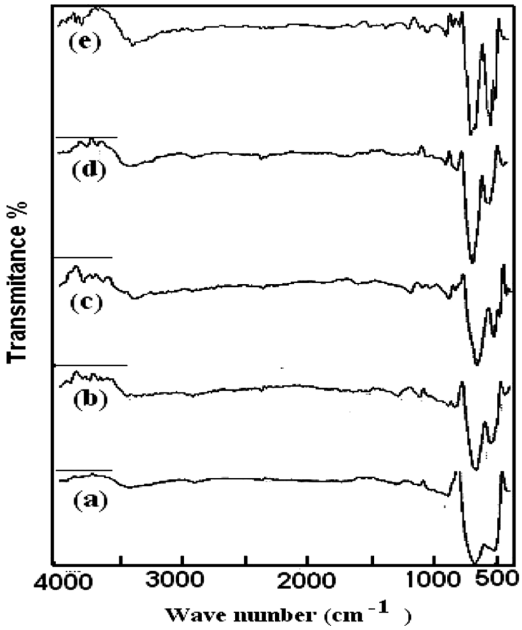

Figure 3: FTIR spectra of different supported samples of CuO/TiO_2: 0.5CuT (a), 2CuT (b), 8CuT (c), 15CuT (d) and 20CuT (e).

of TiO_2 surface and edges with CuO particles. The particle sizes of CuO/TiO_2, measured from TEM image, are in the range of 50–140 nm.

Surface Texture of the Investigated Catalyst Samples

Nitrogen adsorption-desorption isotherms at 77 K for all samples shown in Figure 5(A) are of type II of BDDT's classification [20,21]. All isotherms exhibit narrow hysteresis loops, except for 0.5CuT sample (curve b) whose isotherm is completely reversible. The isotherm of parent TiO_2 sample (curve a) and those for TiO_2 with low CuO loadings (2CuT and 8CuT), have hysteresis loops closing at high relative pressure, P/Po ~ 0.85; (curves c and d). The isotherms of high loadings (15CuT and 20CuT), show somewhat wider hysteresis loops that closed at medium relative pressure, P/Po ~ 0.6 (curves e and f).

The obtained data of specific surface area (S_{BET}), BET-C constant, total pore volume (V_p) taken at 0.95 P/P_o and average pore radius (r^{-cp}) assuming cylindrical pore model for which the superscript (cp) is used, are summarized in Table 1. Obviously, the specific surface area (S_{BET}) of the parent TiO_2 is gradually increased upon increasing the CuO loading up to 15 wt%, but decreased with the highest CuO loading (20CuT sample). This was accompanied by parallel gradual narrowing of the pore radius reaching its minimum values, $r^{-cp} \sim 3.2$ nm for 15CuT sample followed by some pore radius widening for the 20CuT sample.

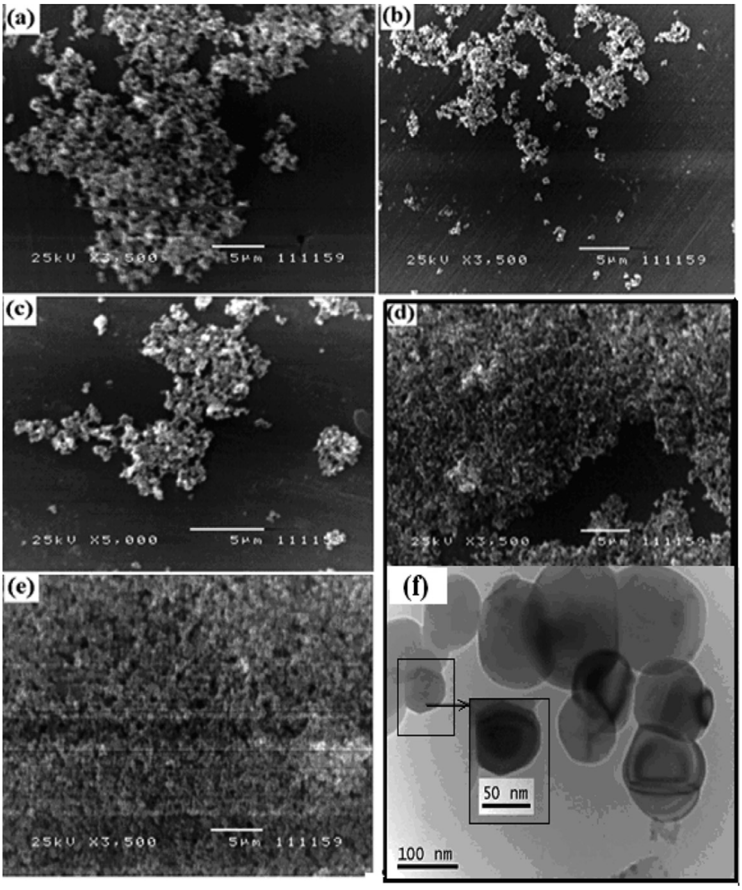

Figure 4: SEM micrographs of parent TiO_2 (a) and different supported CuO/TiO_2 samples: 0.5CuT (b), 2CuT (c), 8CuT (d), 15CuT (e) and TEM micrograph of 8CuT (f).

For pore structure analysis, V_l-t plots were constructed, where V_l is the amount of adsorbed N_2 in ml/g and t is the statistical thickness in Å. In the present study, the reference t-curves of [22–24] based on nonporous solids were adopted according to the C_{BET} values of the samples. The agreement between the values of S_{BET} and S_t (Table 1) ensured the correct choice of the reference t-curves.

The V_l-t plots shown in Figure 5(B), generally show upward deviation with continuous increasing slope till the saturation pressure was attained, for the parent TiO_2 and the other xCuT samples of different CuO loadings. This indicates the predominance of wider pores, which become narrower as the CuO loading percent increase, due, most likely, to the insertion of a larger fraction of CuO species into the titania pore system. It can thus be concluded that a fraction of loaded CuO exists on the titania external surface, while a larger fraction seems to be inserted into the pore system, especially above the monolayer formation [17].

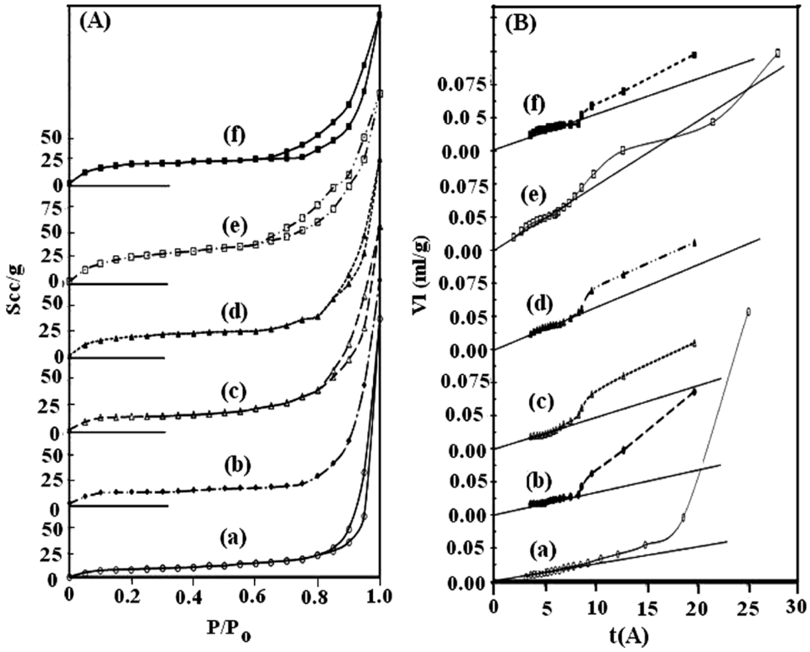

Figure 5: (A) N_2 adsorption – desorption isotherms, (B) V_l-t plots, of: pure titania (a) and CuO/TiO$_2$ samples: 0.5CuT (b), 2CuT (c), 8CuT (d), 15CuT (e) and 20CuT (f).

Performance of the Catalyst Samples in Bulk Polymerization of MMA

Table 2 shows the %conversion of MMA in the presence of pure TiO$_2$, pure CuO and the 8CuT sample with or without oxygen during bulk polymerization for 5 h at 80°C, without cocatalyst or initiator. In all experiments, the catalyst – monomer ratio was 2.5% w/w (0.06 g catalyst and 2.8 g monomer). Pure CuO had an inhibiting effect on the polymerization process with and without O$_2$. The detectable increase in %conversion upon using O$_2$ instead of N$_2$, namely

Table 2: %Conversion of MMA in the presence of pure TiO$_2$, pure CuO and 8CuT with or without oxygen and MMA only at 80°C and after 5 h.

Runs	%Conversion
MMA only	0.1
Pure TiO$_2$	20.0
Pure TiO$_2$ + Oxygen	24.2
Pure CuO	−ve
CuO + Oxygen	−ve
8CuT	67.9
8CuT + Oxygen	75.4

Table 3: Catalytic activity of various supported CuO/TiO_2 samples in bulk polymerization of MMA and characteristic parameters of the produced polymers.

				Tactospecificity					
XCuT	%Conversion	$\overline{Mw}$ ($\times 10^{-5}$)	$\overline{Mw}/\overline{Mn}$	I (mm)	H (mr)	S (rr)	pentads	β	α
0.5CuT	25.6	3.28	4.83	4.3	33.9	45.8	16.0	0.7	2.7
2CuT	32.3	3.47	3.99	4.4	33.0	44.6	18.0	0.7	2.7
8CuT	67.9	5.96	3.15	4.4	34.7	47.2	13.6	0.7	2.7
15CuT	41.8	4.15	4.42	4.2	33.5	46.0	16.3	0.7	2.8
20CuT	33.1	7.16	4.77	4.3	34.0	46.4	15.3	0.7	2.7

*Pentads (mmmr or rmmr) in % estimated at 1.27 ppm in the ^{1}HNMR spectra (26).
*I: isotacticity, H: heterotacticity and S: syndiotacticity (ratios in %).

of 4.2% with pure titania and 7.5% with a 8CuT sample, may point to the possibility of an oxidative polymerization route in these cases. Moreover, the increase in %conversion of ~55.4% upon supporting CuO on TiO_2 reveals clearly the stabilized favorable interaction between CuO and TiO_2.

Table 3 shows the catalytic activity of various supported CuO/TiO_2 samples in bulk polymerization of MMA in a N_2 atmosphere together with the characteristic parameters of the produced polymer. It is clear from Table 3 that increasing the CuO loading up to 8.0 wt% (approaching the monolayer formation [17]), could lead to the highest polymer yield (i.e., 67.9%), and relatively high molecular weights ($\overline{Mw}$ and $\overline{Mn}$), although wide molecular weight distributions (WMWD) were observed in all cases ($\overline{Mw}/\overline{Mn} \gg 1$). Above 8.0% loading, the %conversion decreased which accompanied with wider molecular weight distribution.

The catalyst activity parameter [A] (polymer yield %), is plotted against the fractional degree of coverage of the titania surface with Cu ions [α^{2+}_{Cu}], taking the cross-sectional area of one Cu^{2+} ion, σ^{2+}_{Cu}, as $2.37 \times 10^{-20}\,m^2$ [14]. The obtained logarithmic plot shown in Figure 6, fits an empirical equation of the type: $\log[A] = a + b \log \alpha^{2+}_{Cu}$, where the constants a and b are 0.1352 and 1.3727 a.u., respectively. This plot may suggest that the catalytic behavior of the CuT system in the bulk polymerization of MMA is strictly dependent on the distribution mode of surface CuO species and their interaction with TiO_2 surface, following the same mechanism on all samples under study.

Stereoregularity and Tacticity Statistics of the Produced Polymers

Referring to Table 3, it is clear that the polymers produced in the presence of xCuT catalyst samples of different loadings show predominating syndiotactic-structures. It is noticed that all the polymers produced in the presence of different CuO loadings had almost the same characteristics, namely tactospecificity

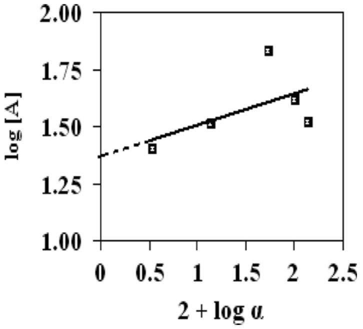

Figure 6: The logarithmic relationship between the catalyst activity parameter (A), and the fractional degree of surface coverage (α).

(mm : rm : rr ratios) and polydispersity ($\overline{M}w/\overline{M}n$, being >1). For 8CuT, a little loss in pentads % (mmmr or rmmr appeared at 1.27 ppm in the ^{1}H NMR spectra [25]) seems to be linked with higher $\overline{M}w$ values as a function of the mode of enchainment.

On the other hand, the β values (i.e., 4[mm][rr]/[mr]^2) of syndiotactic polymers produced in all cases are close to 1, indicating most probably the chain-end control mechanism [13,26]. The α values (i.e., 2[rr]/[mr]) of the produced polymers are markedly far from 1, revealing no enantiomorphic-site control approach [13,26]. One may thus conclude that the enchainment is most likely catalyst-controlled depending on the mode of CuO-TiO_2 interaction. The high stereospecific nature of the produced polymer in all cases can be attributed to the titania support effect, being activated by dispersing copper oxide on its surface and/or to the mode of interaction between CuO phase and surface titania (external surface and/or its pore system) [14].

Suggested Mechanism of Polymerization Process

Based on the guide bulk polymerization experiments in the presence of O_2, it was assumed that the oxidative polymerization route is favored at the studied conditions. The conduction band electrons of TiO_2 can reduce O_2 to free radicals [27] that can participate in the initiation and propagation step, in pure TiO_2 and the supported sample (8CuT). In the absence of oxygen, however, where the role of CuO, TiO_2 and their interaction mode were to be considered, a redox route of the reaction could be suggested. This should be encouraged by the excess oxygen in the CuO-nonstoichiometric lattice structure as well as by the presence of trapped electrons in the weighted distorted conduction band of TiO_2, assuming the preparation conditions can allow the n-p junction to be operated between the two phases (CuO and TiO_2) especially by thermal treatment. One may expect that the e^-_{CB} (the available electrons in TiO_2) being involved in the interaction, can be transfered to Cu^{+2} [2,28,29]. This transfer of electrons is also favored by the polymerization reaction conditions. The redox-initiated mechanism of the polymerization process may thus proceeds as follow:

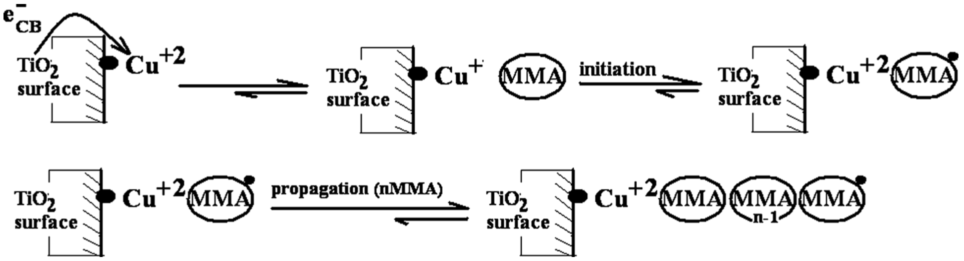

CONCLUSION

The study from different angles of the interaction mode between CuO and TiO_2 has shown that the characteristics of the produced catalyst system may be used successfully in redox-initiated polymerization of MMA.

REFERENCES

[1] Xu, S., and Sun, D. D. *Intern. J. Hydrogen Energy* **34**, 6096 (2009).

[2] Slamet, Nasution, H. W., Purnama, E., Riyani, K., and Gunlazuardi, J. *World Appl. Sci.* **6**, 112 (2009).

[3] Yang, S., and Lian, G. *J. Am. Ceram. Soc.* **88**, 968 (2005).

[4] Hayashi, H., and Torii, K. *J. Mater. Chem.* **12**, 3671 (2002).

[5] Kraeutler, B., and Bard, A.J. *J. Am. Chem. Soc.* **100**, 5985 (1978).

[6] Rao, M.V., Rajeshwar, K., Vernekar, V.R.P., and DuBow, J. *J. Phys. Chem.* **84**, 1987 (1980).

[7] Martin, C., Rives, V., and Sanchez-Escribano, V. *Surf. Sci.* **251–252**, 825 (1991).

[8] Raghuraman, G. K., Rühe, J., and Dhamodharan, R. *J. Nanopart. Res.* **10**, 415 (2008).

[9] Zhang, H., and Banfield, J. F. *J. Phys. Chem. B.* **104**, 3481 (2000).

[10] Feng, L. "Preparation and Characterization of Polymer TiO_2 Nanocomposites Via In-situ Polymerization," Thesis, Master of Applied Science in Chemical Engineering, University of Waterloo, Waterloo, Ontario, Canada, 2006, © Feng Lin (2006).

[11] Moustafa, A. B., and Abd-El-Hakim, A. A. *J. Appl. Polym. Sci.* **21**, 905 (1977).

[12] Sing, K. S. W., Everret, D. H., Haul, R. A. W., Moscou, L., Pierotti, R. A., Rouquerol, J., and Siemieniewska, T. *IUPAC, Pure Appl. Chem.* **56**, 603 (1985).

[13] Sadek, E. M., Mekewi, M. A., Yehia, F. Z., Solyman, S. M., and Hassan, S. A. *Macrom. Chem. Phys.* **202**, 1505 (2001).

[14] Hassan, S. A., Selim, S. A., Mekewi, M. A., and Hanafi, S. *J. Mater. Sci.* **24**, 1095 (1989).

[15] Solyman, S. M., and Badawi, A. M. 4th International Conference on Chemical & Environmental Engineering 27–29 May, Cairo, Egypt, p. 66 (2008).

[16] Muhamad, E. N., Irmawati, R., Abdullah, A. H., Taufiq-Yap, Y. H., and Abdul Hamid, S. B. *The Malaysian J. Analy. Sci.* **11**, 294 (2007).

[17] Xiao-Feng, Y., Nian-Zu, W., You-Chang, X., and You-Qi, T. *J. Mater. Chem.* **10**, 1629 (2000).

[18] Huang, J., Wang, S., Zhao, Y., Wang, X., Wang, S., Wu, S., Zhang, S., and Huang, W. *Catal. Commun.* **7**, 1029 (2006).

[19] Hassan, S. A., Mekewi, M. A., Shebl, F. A., and Sadek, S. A. *J. Mater. Sci.* **26**, 3712 (1991).

[20] Emmett, P. H., and Brunauer, S. *J. Am. Chem. Soc.* **59**, 1553 (1937).

[21] Brunauer, S., Deming, L. S., Deming, W. E., and Teller, E. *J. Am. Chem. Soc.* **62**, 1723 (1940).

[22] Carruthers, J. D., Cutting, P. A., Day, R. E., Harris, M. R., Mitchell, S. A., and Sing, K. S. W. *Chem. & Ind.* 1772 (1968).

[23] Payne, D. A., and Sing, K. S. W. *Chem. & Ind.* 918 (1969).

[24] Cransten, R. W., and Inkley, F. A. *Advanc. Catal.* **9**, 143 (1957).

[25] White, A. J., and Filiko, F. E. *J. Polym. Sci.: Letter Ed.* **20**, 525 (1982).

[26] Ewen, J. A. *J. Am. Chem. Soc.* **106**, 6355 (1984).

[27] Sobczyński, A., and Dobosz, A. *Polish J. Environ. Stud.* **10**, 195 (2001).

[28] Paola, A. D., Augugliaro, V., Palmisano, L., Pantaleo, G., and Savinov, E. *J. of Photochem. and Photobiol. A: Chem.* **155**, 207 (2003).

[29] Chiang, K., Amal, R., and Tran, T. *Adv. Environ. Res.* **6**, 471 (2002).